SURFACE IMPEDANCE OF INDIUM IN A MAGNETIC FIELD PERPENDICULAR TO THE SURFACE OF THE METAL

P. P. KRYLOV

Institute of Physics Problems, USSR Academy of Sciences

Submitted February 9, 1968

Zh. Eksp. Teor. Fiz. **54**, 1738—1755 (June, 1968)

The dispersion law and damping of helical plasma waves (helicons) and the radio-frequency size effects in a magnetic field H perpendicular to the surface of single-crystal In plates are investigated. The experiments were carried out at helium temperatures, and a modulation technique was used to measure the derivative of the imaginary part of the surface impedance. On the basis of available data on the In Fermi surface it was found that the helicon-absorption edge at a certain field H_e is not determined by the limiting-point electrons, but by electrons of other extremal cross sections, the characteristics of which were determined from the experimental data. Landau damping was observed in the course of the study of the dependence of the helicon amplitude on the magnetic-field direction. Impedance oscillations periodic with respect to the field strength were observed at fields $H < H_e$. They depend on the number of revolutions executed by the electrons on moving between opposite surfaces of the plates. The experiments showed that the oscillation amplitude is maximal if the displacement of the electrons towards the interior of the metal per revolution is comparable to the depth of the skin layer. Short-period oscillations were observed in low fields. Possible causes of their appearance are discussed. Besides the oscillations due to ineffective electrons, narrow lines from effective electrons were observed in weak fields.

IN a constant magnetic field H perpendicular to the surface of a metal, the electrons move into the interior of the metal along helical trajectories. The pitch of each helix is equal to the displacement of the electron during the cyclotron period T:

$$u = \bar{v}_H T = \frac{c}{eH} \frac{\partial S}{\partial p_H}.$$

Here $\bar{v}_H$ is the average component of velocity along H, $S = S(p_H)$ is the area of the intersection of the Fermi surface with the plane p_H = const, and p_H is the projection of the electron quasimomentum on the direction of the field H. The maximum of the quantity u as a function of p_H will be denoted u_{max}. In a metal with a spherical Fermi surface, the largest displacement $u = u_0 = 2\pi c p_f / eH$ is possessed by electrons of the limiting points (p_S—Fermi momentum).

In a sufficiently strong field, when the cyclotron period of the electrons is small compared with the relaxation time, helical plasma waves—helicons[1,2] can propagate in an uncompensated metal. In the case of a metal with a singly-connected Fermi surface and a carrier density N, the dispersion law of the helicons propagating along H has the simple form

$$k^2 = 4\pi Ne\omega / cH, \tag{1}$$

(k—wave vector, ω—frequency of electromagnetic field). Relation (1) is valid if the inequality $ku_{max} \ll 1$ is satisfied (local limit). In the region $ku_{max} \geq 2\pi$ the energy of the alternating field is resonantly absorbed by the group of electrons from which $ku = 2\pi$ (Doppler-shifted cyclotron resonance). The absorption can be so strong that in fields smaller than a certain threshold value H_e the helicons do not exist as excitations with a definite value of k. For the Fermi sphere, the field of the absorption threshold H_e is determined by the condition $ku_0 = 2\pi$. The absorption threshold of helicons was observed in polycrystalline Na, K, In[3] and in single-crystal Al[4] and Cu[5].

At $H < H_e$, the electromagnetic field can penetrate into the metal as a result of the motion of individual groups of electrons (see, for example, the review[6]). Connected with this anomalous penetration are the corresponding size effects. In the presence of the so-called effective electrons, which move in individual sections of the trajectory parallel to the surface, a system of peaks of high-frequency fields and currents is produced in the metal, and the distance between them in depth is determined by the characteristic dimensions of the trajectories. Weaker effects of anomalous penetration are connected with electrons whose velocity projection on the normal to the surface does not vanish anywhere. A unique standing helical wave may be produced in the metal, with a spatial period that does not depend on the frequency of the exciting field and is determined by the electron displacement u. An oscillating term, connected with the number of revolutions executed by the electrons on the path from one surface of the sample to the other, appears in the dependence of the impedance of a plane-parallel plate on H. Oscillations of this type, which are periodic in the dc field, were first observed in Sn[7] and quite recently in single crystals of Cu[5].

In the present paper we investigated effects occurring in single-crystal In at low temperatures and connected with excitation of plasma waves as well as radio-frequency size effects in a normal field, due to the motion of both effective and ineffective electrons. We were able to establish that the absorption threshold for helicons and the oscillations of the size effects are determined by different groups of electrons, which are not the electrons of the limiting points in either case. The

Sample	Orientation of normal	Direction of E	Thickness mm	H_e, kOe, at 1 MHz	ΔH_α, kOe	ΔH_β, kOe	H_γ, kOe	u/u_0 calculated from the data on			
								w_e	H_e	ΔH_α	H_γ
1	$\sphericalangle$([001], **n**) =2°	[100]	0.40	16.6	0.70	0.38	—	—	0.77	0.45	—
1'	$\sphericalangle$([001], **n**) =3°	[100]	0.29	16.5	0.93	0.30	1.30	0.76	0.76	0.43	0.60
1''	$\sphericalangle$([001], **n**) =5°	[110]	0.20	16.7	1.45	0.47	2.05	—	0.78	0.46	0.65
2	$\sphericalangle$([100], **n**) =2°	[010]	0.40	17.5	—	—	—	—	0.79	—	—
$2_1'$	$\sphericalangle$([100], **n**) =4°	[011]	0.30	18.0	—	—	1.50	0.82	0.82	—	0.72
$2_2'$	$\sphericalangle$([100], **n**) =4°	[010]	0.30	18.0	—	—	1.50	0.82	0.82	—	0.72
3_1	$\sphericalangle$([110], **n**) =4°	[1$\bar{1}$0]	0.29	15.0	1.15	—	—	0.82	0.75	0.53	—
3_2	$\sphericalangle$([110], **n**) =4°	[001]	0.29	15.0	1.20	0.20	—	—	0.75	0.56	—
3'	$\sphericalangle$([110], **n**) =7°	[001]	0.30	14.8	1.15	0.20	—	—	0.73	0.55	—
4	$\sphericalangle$([011], **n**) =2°	[100]	0.30	14.7	1.02	0.34	—	0.71	0.69	0.49	—
5	$\sphericalangle$([111], **n**) =2°	[2$\bar{1}\bar{1}$]	0.50	8.5 *	1.2	—	—	—	0.31	1.0	—
5'	$\sphericalangle$([111], **n**) =2°	[2$\bar{1}\bar{1}$]	0.30	9.2 *	0.33	—	—	0.37	0.35	0.16	—
Error	0.5°		—	2%	up to 5%			5%		7%	

*The given value is that of H_{min}.

dispersion and damping of the helicons were investigated not only for the case H ∥ k, but also for different angles ψ between H and k (up to 45°). At the same time, we determined the role of the Landau damping, which governs to a considerable degree the dependence of the amplitude of the helicons in the anisotropic metal on the direction of the magnetic field. In the analysis of the experimental results, we made use of the known data on the Fermi surface of In, which by now has been sufficiently well studied[8,9].

EXPERIMENT

The experiments were performed at helium temperatures and consisted of measuring the dependence of the derivative of the imaginary part of the surface impedance Z = R + iX of single-crystal In plates on the magnetic field. In the experiments we used the same procedure for measuring $\partial X/\partial H$ and for preparing the samples as was used for the investigation of the radio-frequency size effect in a parallel field[10]. In place of the previously employed large-diameter discs, we use relatively narrow strips of width ≈ 3 mm, in view of the need for modulating in the sample a magnetic field perpendicular to its surface. (The modulation frequency was 20 Hz.) Control experiments with samples of different width allow us to state that the possible incomplete penetration of the modulating field in the sample exerted no noticeable influence on the investigated effects. It turned out to be possible to cut samples of the required form by means of a blade out of single-crystal discs, for as a result of such an operation the amplitude of the size-effect lines remained essentially unchanged. (It can be assumed that, just as in the preceding experiments, the mean free path of the electrons is $l \approx 0.5$ mm at T = 1.3° K[11]). Apparently mechanical stresses in our samples were negligible, owing to the annealing that took place even at room temperatures.

The main characteristics of the samples are listed in the table. We investigated samples of five different crystallographic orientations of the normal **n** to the surface of the sample. The influence of the polarization of the external high-frequency field **E** was investigated on strips cut from the same disc in different directions. These samples are designated in the table by different indices. The primes denote samples having approximately the same orientation of the normal, but different thickness d. The lengths of the strips were varied in the range 10–18 mm.

The sample was placed in the inductance coil of an oscillator tank circuit, as shown schematically in Fig. 1. To cover the frequency range 0.12–14 MHz, three interchangeable coils were used. The coils were glued on a teflon or polystyrene holder and immersed in liquid helium either directly or inside a vacuum-type vessel with heat-exchange gas, since the boiling of the helium in the coil above the λ point greatly increased the oscillator noise, owing to the increase in the relative capacitance fluctuations, when the tests were made at high frequencies. The magnetic field, which was oriented horizontally, was produced by an electromagnet and was varied in the interval 0–22 kOe. The sample together with the cryostat could be rotated about the axis through an angle. At the same time, the instrument could be inclined in the vertical plane passing through H through an angle up to ± 8°.

The sensitivity of the setup made it possible to discern nuclear resonance signals on protons and F nuclei in the teflon and on Cu nuclei in the wire of the coil. With the aid of these signals, and also with the aid of a special nuclear-resonance pickup, we calibrated the Hall pickup, whose voltage was fed to the x coordinate of an automatic x-y plotter. The total x-coordinate error, including the errors of the Hall pickup and of the automatic plotter, was ≈ 2%.

A typical plot of $\partial X/\partial H$ in a magnetic field perpendicular to the surface of the In plate is shown in Fig. 2. We can separate on the curves three frequency-dependent magnetic-field ranges, in which different phenomena have been observed: helicons, periodic oscillations (henceforth denoted by the letter α), and short-period oscillations (β). In addition to these oscillatory size effects, we observed in certain samples in weak fields also narrow size-effect lines due to the effective electrons (see Fig. 14 below). We shall first report the re-
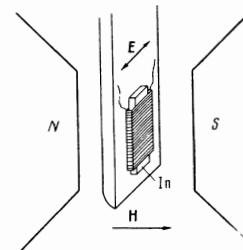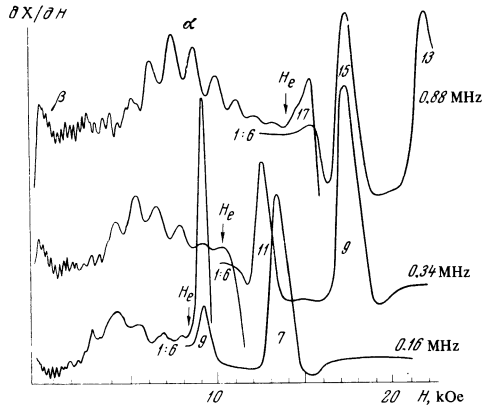

FIG. 1.

FIG. 2. Plot of the derivative of the surface impedance of sample 3_2 at H ∥ [110] and t = 1.4°K. In plotting the helicons, the sensitivity was decreased by a factor of 6. Under the resonant maxima are indicated the number of half-waves subtended by the plate (number of resonance) and the right sides of the curves show the frequency of the electromagnetic field. The arrows denote the helicon absorption threshold fields.

FIG. 3   FIG. 4

FIG. 3. Plot of n'^2 against the reciprocal field at H ∥ [110]. ●—experimental results for sample 3_1, O—for sample 3_2. The horizontal lines correspond to a local dispersion law. The inclined lines are marked by the values of the frequencies at which the corresponding experimental points were obtained. The line $ku_{max} = 2\pi$ corresponds to the value $u/u_0 = 0.64$ obtained from the model of almost free electrons.

FIG. 4. Deviations from local dispersion for H parallel to the indicated crystallographic axes, obtained for samples 1', 2', 3_2, and 4. Different numbers of the resonances correspond to different symbols: ⊙—n = 5, △—n = 7, O—n = 9, □—n = 11, X—n = 13, ◇—n = 15, ▽—n = 17. The black points in the upper diagram show data obtained with sample 1. In the diagram for H ∥ [100], the black points denote the results of an investigation of helicons propagating along [110] (sample 3_1). For the sake of clarity, the characteristic points indicate the error, equal to 4% along the abscissa axis and 6% along the ordinate axis. The error includes the systematic error of measurement of the sample thickness.

sults on the helicons, and then on the radio-frequency size effects.

HELICONS

1. Resonance maxima of ∂X/∂H, corresponding to excitation of standing helical waves in the plate, were observed for all samples in fields stronger than a sudden threshold field H_e, which depended on the frequency and orientation of the normal. In our experiments, the magnetic components of the external field were aligned in the same direction on opposite surfaces of the plates, and the electric components E in opposite directions. With such an excitation, ∂X/∂H reaches a maximum when an odd number of half-waves n is spanned by the plate thickness, i.e., k = $\pi n/d$[1]. Strictly speaking, the resonances should shift as a result of the finite transverse dimensions of the sample. In most samples, the ratio of the thickness to the width of the strip does not exceed 0.10. According to the theory of Legendy[12], at such a ratio of the plate dimensions the shift of the resonances with numbers n ≥ 5 is less than 0.5%. However, the theory developed in[12] pertains to the case kl ≪ 1, whereas in our experiments kl ≫ 1. Therefore the absence of a noticeable shift of the resonances was verified experimentally and experiments with samples of different thickness and in a control experiment with a wide sample (≈ 9 mm wide) comes from the same disc as sample 1'. Within the limits of the field measurement errors, the position of the peaks on the broad sample, compared with sample 1', remained unchanged. The final value of the damping shifts the resonance by a negligibly small amount.

To obtain information concerning the helicon dispersion law, we have traced the dependence of the position of the resonant peaks on the frequency of the electromagnetic field. The results obtained for one of the crystalline orientations of the normal are shown in Fig. 3, where the ordinates represent the quantity $n'^2 = 4Ned^2\omega/\pi cH$. If the local dispersion law (1) is valid, then the quantity n' = 1 is simply the number of the resonant peak. We chose for ln the value N = 3.93
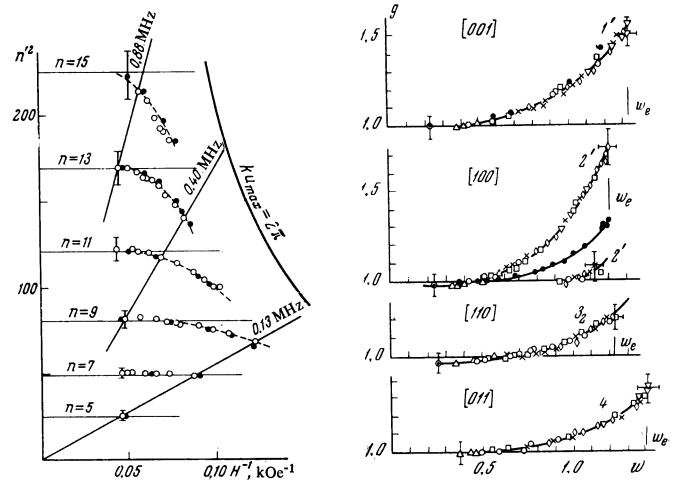
× 10^{22} cm^{-3}, corresponding, with allowance for the temperature contraction, to a carrier density of one hole per atom. This is justified by the results of measurements of the Hall constant with the aid of low-frequency helicons, where a value of N close to the theoretical one was obtained[13,14]. From plots similar to that shown in Fig. 3, it is clear that the local dispersion law (1) is satisfied in the region $ku_{max} ≪ 2$.

With increasing field and on approaching H_e, a deviation from the local dispersion law is observed. This deviation is characterized on the plots of Fig. 3 by a deviation of the experimental points from the horizontal straight lines. For short waves in the investigated range of fields, it is impossible to come sufficiently closely to the limiting value $n'^2 = n^2$. It is possible, however, to determine consecutively the number of each resonant peak, starting from the fully determined number n for the preceding resonances.

For free electrons, the deviation from the local dispersion law (1) under the conditions kl ≫ 1 is described by a certain function of the variable w = $ku_0/2$, so that the dispersion law can be written in the form

$$k^2 = \frac{4\pi Ne\omega}{cH} f(w).$$

For a standing wave w = $\pi p_f cn/eHd$. When w ≪ 1, we have f(w) ≈ 1. The threshold field H_e is determined by the condition w = 1, f(1) = 1.5 in the limit as kl → ∞. An
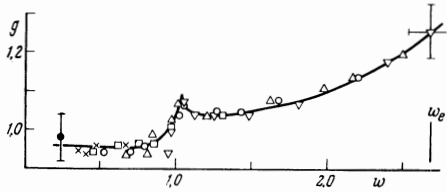
FIG. 5. Deviation from local disperson law for the orientation **H** ‖ [111], sample 5'. ●—n = 5, X—n = 7, □—n = 9, ○—n = 11, △—n = 13, ▽—n = 15.

analytic expression for f(w) is presented, for example, in [3,15].

To describe the dispersion of helicons in In it is possible to introduce a function g analogous to f(w). As a final result of the reduction of the experimental results, Figs. 4 and 5 show the quantity $g = n^2/n'^2$ as a function of w. By p_f in the expression for w we mean the radius of the Fermi surface moving in the model of almost free electrons, $p_f = 1.10p_0 = 1.60 \times 10^{-19}$ g-cm/sec, $p_0 = 2\pi\hbar/a$ is the end-point momentum of the Brillouin zone in the [100] direction (a—lattice constant at helium temperatures). The function g characterizes directly the conductivity tensor $\hat{\sigma}$, which depends on the wave vector. If we direct the z axis along **k** ‖ **H** and put $\sigma_- = \sigma_{xy} - i\sigma_{xx}$, then for an axially-symmetrical Fermi surface we have

$$g = \frac{\operatorname{Re} \sigma_-(k, H)}{\operatorname{Re} \sigma_-(0, H)},$$

where $\sigma_-(0, H) = Nec/H$ as $l \to \infty$ (see, for example, [4,15]). The Fermi surface of In does not have rotational symmetry. In the general case this leads to the appearance of longitudinal components σ_{xz} and σ_{yz} in the conductivity tensor, and calculation of the spectrum of the plasma waves becomes quite complicated. It is interesting that, in accordance with the experimental data, in spite of the complicated form of the Fermi surface of In, the deviations from the local dispersion law are described for each orientation of **H** by a function of a single parameter w.

According to the results of [8,9], the hole surface of In in the second zone is close to the model constructed in the almost-free-electron approximation (see Fig. 6). Figure 7 shows the dependence of the quantities u/u_0 and T/T_0 on p_H for this model. Here $T = T(p_H)$ is the cyclotron period for electrons having a specified value p_H; T_0 is the cyclotron period of the free electrons. In our approximation T/T_0 is simply the sum of the angular dimensions of the arcs making up the orbit, divided by 2π. In the calculation of $u(p_H)$, each term in this sum must still be multiplied by a corresponding component z_H.

The maximum displacement along the field $u = u_0$ at **H** ‖ [001] or **H** ‖ [100] is possessed by the electrons of the limiting points on the corresponding square "cups." We have, however, observed resonant peaks of helicons at w > 1. In the direction of the [111] axis on the Fermi surface of the second band there is a large spherical section with a curvature radius equal to p_f[11], which causes a noticeable increase of the damping of the helicons at w ≈ 1. Accordingly, the electrons of the limiting points influence also the dispersion law when **H** ‖ [111].
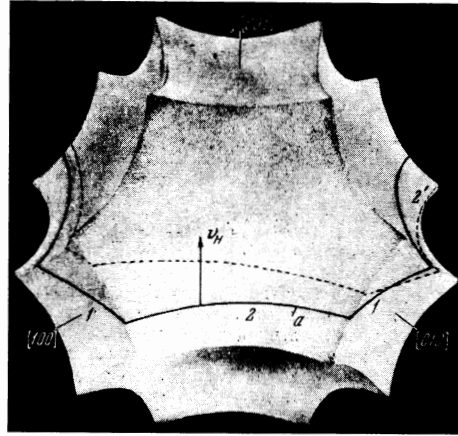

FIG. 6. Fermi surface of In in the second band: a—section at **H** ‖ [001], causing the γ-lines.

The plot of g(w) (Fig. 5) shows clearly the singularity at w = 1. It must be emphasized, however, that the resonant peaks were traced far into the region of w > 1. Thus, in this case, just as when **H** ‖ [001] or **H** ‖ [100], it can be stated that the threshold of helicon absorption is not determined by the limiting points.

In this connection, we must make the following remark. The hole Fermi surfaces for Al and In are very similar. In[4] it is concluded that the helicon absorption threshold in Al when **H** ‖ [100] is due to electrons of the limiting point. Apparently, the small mean free path of the electrons, and possibly the insufficient sensitivity of the apparatus, did not make it possible to observe helicons in Al at w > 1.

We were unable to observe the peak of the Doppler-shifted cyclotron resonance, similar to that observed in alkali metals[3]. The only distinct minimum of $\partial X/\partial H$ in a certain field $H_{min} \propto \omega^{1/3}$ (see the table) was observed for **H** ‖ **n** ‖ [111]. However, we always observed a sufficiently sharp helicon absorption edge. We assumed H_e to be the value of the field at which the kink of $\partial X/\partial H$ is observed. This field is designated by an arrow on three characteristic plots of $\partial X/\partial H$ in Fig. 2. For the threshold field determined in this manner, a dependence $H_e \propto \omega^{1/3}$ was observed for all samples, in accordance with the theory[3,15] (an example for one of the orientations is shown in Fig. 8). The table lists all the values of H_e,
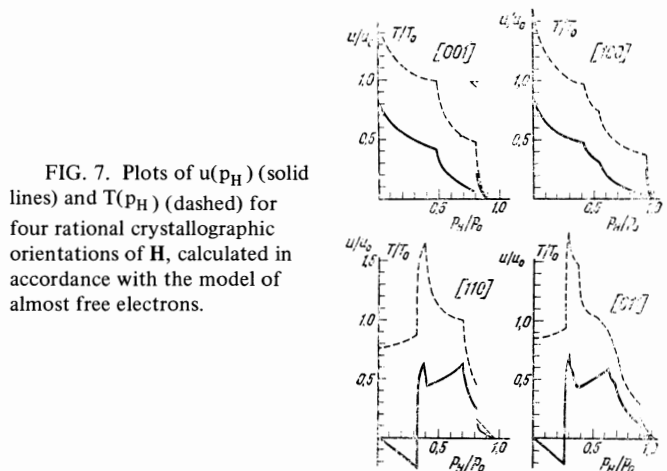

FIG. 7. Plots of $u(p_H)$ (solid lines) and $T(p_H)$ (dashed) for four rational crystallographic orientations of **H**, calculated in accordance with the model of almost free electrons.

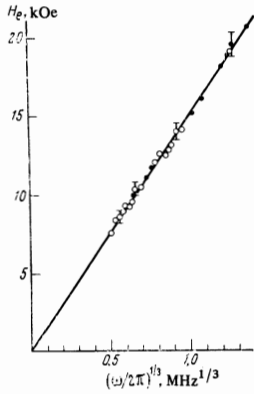FIG. 8. Plot of H_e against the frequency: ●—sample 3_1, ○—sample 3_2. The vertical segments indicate the uncertainty in the choice of H_e.

FIG. 9   FIG. 10

FIG. 9. Plots of $\partial X/\partial H$ at $H \parallel [100]$; sample $2'_1$, $T = 1.4°K$. The curves are marked with the frequency of the electromagnetic field and the number of the resonance. In strong fields, quantum oscillations are seen, with an amplitude that is strongly reduced by the large rate of change of the field.

FIG. 10. Frequency dependence of the positions of the extrema. The dashed lines show the frequency dependence of the field H_e, designated by the arrow on the plots of Fig. 9. The black points correspond to maxima in the fields $H_{\tilde{n}} < H_e$, the light points correspond to a smeared maximum in fields $H_{\tilde{n}} < H_e$. The straight lines correspond to a local dispersion law. The numbers of the resonants are indicated on the right.

referred to a frequency of 1 MHz. It is obvious that, owing to the finite mean free path, the absorption edge becomes smeared out. This leads to an uncertainty in the choice of H_e, as indicated by the vertical segments for several points in Fig. 8.

For the group of electrons governing the helicon absorption threshold it is possible to determine u/u_0 in two ways. First, the condition $ku/2\pi = uw/u_0 = 1$ makes it possible to estimate u/u_0 directly, by choosing for u the maximum value of w_e noted in Figs. 4 and 5. Second, using the experimental values of $g_e = g(w_e)$, we can calculate u/u_0 from the relation

$$H_e{}^3 = \left[\frac{4\pi N p_f{}^2 c}{e}\right]\left(\frac{u}{u_0}\right)^2 g_c\omega,$$

where the factor in the square brackets is determined completely by the In crystal lattice constant[2]. For H oriented parallel to the directions $[001]$, $[100]$, and $[011]$, the values of u/u_0 obtained by these two essentially equivalent methods agree within the limits of the measurement error of the magnetic field. (See the table; the values of u/u_0 obtained from the values of w_e are presented for those samples for which the helicon dispersion law near threshold was investigated in greatest detail). Comparison of the experimental values of u/u_0 with the plots of Fig. 7 shows that the helicon absorption threshold is determined by the cross sections with the largest value of the displacement $u = u_{max}$, if one excludes from consideration the electrons of the limiting points. For the orientations $H \parallel [001]$ or $H \parallel [100]$ the displacement u_{max} is possessed by orbits of type a on Fig. 6, which are very close to the central section.

For the orientation $H \parallel [110]$, there is a discrepancy between the experimental values of u/u_0 obtained by different methods. In addition, the model of almost free electrons gives a much lower value of u_{max}. In this case, on approaching H_e, the attenuation apparently increases more strongly than for other orientations, and the resonant maxima are not observed already at $ku_{max} < 2\pi$. A similar situation with $H \parallel [110]$ was observed in Al[4].

Concluding the results of the study of helicons propagating along a magnetic field, we note that in experiments with samples $2'$ we observed a wave propagating below the absorption threshold of the ordinary helicons. At $H \parallel [100]$ we observed a weak smeared maximum of $\partial X/\partial H$ in fields $H_{\tilde{n}} < H_e$ (see Fig. 9). As seen from the diagrams of Fig. 10, this maximum is due to a wave with nearly local dispersion law. This corresponds to
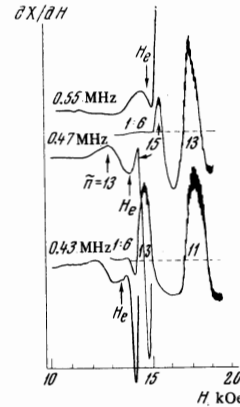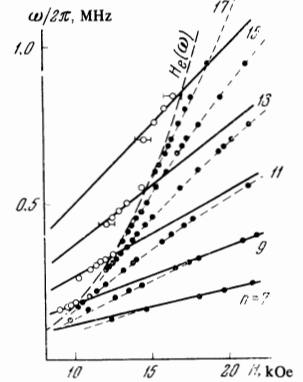
the lower branch of $g(w) \approx 1$ at $w \approx 1$ for the orientation $H \parallel [100]$ on Fig. 4. Obviously this phenomenon is not connected with the helicon spectrum ambiguity indicated in the theory of McGroddy, Stanford, and Stern[16]. It can hardly be explained likewise by the mechanism proposed by Antoniewicz[17], where the propagation of the weakly-damped waves below H_e is due to singularities of the Fermi surface which do not take place in In. We note in addition that the wave dispersion in[17] differs appreciably from the local dispersion (1).

2. Upon variation of the angle ψ between H and K, which is directed along the normal to the surface of the plate, the resonance maxima shifts in accordance with the local theory[1,2], towards larger fields in inverse proportion to $\cos\psi$, provided the condition $ku_{max}/2\pi \lesssim 0.3$ is satisfied. In the opposite case, an appreciable role is assumed by the change of the function g when the orientation of the field H changes. Figure 11a shows plots illustrating the shift of the resonances as a result of the decrease of g when H is rotated relative to $[100]$. The character of the changes occurring following rotation in the planes (101) and (010) is the same and does not depend on the polarization of the external field E. By determining the position of $H \perp n$ from the size effect in a parallel field, and taking into account the deviation of n from $[100]$, we succeeded in establishing that the amplitude of the helical waves is maximal at $H \parallel [100]$. It is possible to verify in the same manner that in sample $1'$, whose angular dependences of the attenuation and of the helicon dispersion are perfectly analogous to the plots of Fig. 11, the maximum of the resonance amplitude is reached at $H \parallel [001]$.

The decrease of the amplitude of the standing plasma waves upon deflection of H from a crystallographic axis
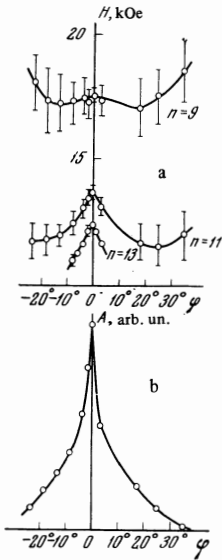
FIG. 11   FIG. 12

FIG. 11. Dependence on the angle φ between H and [100]: a–of the position of the extrema, b–of the amplitude A of the resonance maximum n = 11, obtained for sample $2'_1$; $\omega/2\pi$ = 310 kHz. On the right sides of the curves are marked the numbers of the resonances. The vertical segments show the widths of the resonances at the level shown dashed in Fig. 9.

FIG. 12. Dependence of the helicon amplitude A on the angle φ between H and [110] of helicons: O–n = 9, ●–n = 11. Sample 3_2, $\omega/2\pi$ = 240 kHz. The angle φ = 0 is determined from the maximum of the amplitude n = 9. The small asymmetry of the curves is due to the deviation of the normal from the [110] axis. The lower figure shows the intersection of the (1$\bar{1}$0) plane with the Fermi surface in the second band.

can be attributed to the appearance of Landau damping. This damping mechanism is connected with electrons for which the condition $k\bar{v}_z = \omega$ is satisfied; this condition practically reduces to $v_z = 0$ (the z axis is directed along k, the superior bar over v_z denotes averaging over the cyclotron period). To this should be added the condition $v_z \neq 0$, for if the trajectory of the electrons lies in a plane perpendicular to k, then a wave field of equal magnitude acts on the conduction electron in opposite manner on opposite sections of the trajectory, and the wave absorption is small. If the magnetic field is inclined slightly to the [001] or [100] axis, then a central cross section appears ($v_z = 0$) with a large displacement of the electrons along k on individual sections of the trajectory. As a result, the Landau damping increases and leads to a decrease of the amplitude of the helicons.

We now consider the case of wave propagation along [110] or [011]. As before, the polarization of E is immaterial, but the angular dependences of the damping and dispersion of the helicons are different when H is deflected from the crystallographic axis in different planes. Figure 12 shows plots of the resonance amplitude against the angle φ between the magnetic field and the [110] axis when H is rotated in the (1$\bar{1}$0) plane. The amplitude of the numbers in the region $ku_{max}/2\pi \lesssim 0.7$ (for example, the peak with n = 9 on Fig. 12) greatly decreases at $\varphi = 22°$, corresponding to the angular interval of the existence of a central orbit passing through the square "cups." This can be easily attributed to the
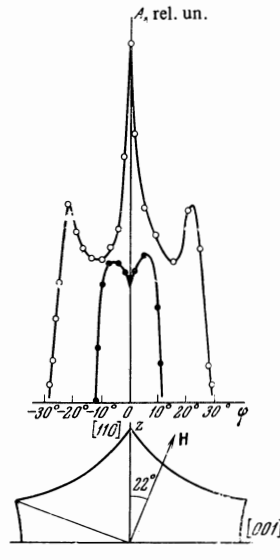
increase of the Landau damping in the case when the central orbit crosses sections of the Fermi surface with large values of v_z. In sample 4, the magnitude of the corresponding angle characterizing the start of the strong helicon damping is much smaller, and amounts to 15°, in full accord with the model of almost free electrons. As to the dependences of the amplitudes on φ for the resonances near H_e (n = 11 on Fig. 12), we are unable to propose a simple qualitative explanation for them, and exact calculations of the helicon damping in the region $ku_{max} \sim 1$ for an anisotropic Fermi surface entail considerable difficulties and have not been made as yet.

When H is rotated in the (001) plane up to an angle $\varphi = 45°$ to the [110] direction, the amplitude of the standing waves remains of the same order as when H ∥ [110]. This is not surprising, if we recognize that in this case the trajectories of the electrons of the central section deviate insignificantly from the plane perpendicular to k. On the other hand, on going through the position H ∥ [100] with increasing φ, these trajectories, roughly speaking, are rotated through 90° and the Landau damping increases abruptly. The amplitude of the resonant peaks drops to zero in the interval φ = 45–48°. The small value of the Landau damping at $\varphi = 45°$ has enabled us to investigate the helicon dispersion law in sample 3_1 at an appreciable value of the angle $\psi \approx 45°$ between the direction of propagation of the wave and H ∥ [100]. For comparison with the data obtained with sample 2', the deviation from the local dispersion law of $g = n^2/n''^2$, where $n''^2 = n'^2/\cos \psi$, was noted on the corresponding diagram of Fig. 4. The abscissa scale was modified with allowance for the value of the angle ψ. The threshold of cyclotron damping is determined by the condition $ku_{max} \cos \psi = 2\pi$. The values of u_{max}/u_0 calculated from the values of w_e or H_e by using the corresponding experimental value of g_e are in full agreement with the data obtained for samples 2 and 3'. From the plots shown in Fig. 4 it is clear that the functions g and, particularly, the value of g_e, depend not only on the crystallographic orientation of the magnetic field but also on the angle between H and k.

3. In the preceding arguments we have tacitly assumed that the characteristics of the plasma waves are determined essentially by the hole surface in the second band. This is justified to some degree by the relatively small number of electrons in the third energy band. The volume of the tubes located in the plane (001) is $\approx$ 5% of the volume of the hole surface. Apparently the helicon absorption threshold can likewise not be determined by the electrons of the third band, owing to the small values of the effective masses and velocities. Estimates of u/u_0 on the basis of the experimental data of Gantmakher and the author[8] and of Mina and Khaĭkin[9] show that $u/u_0 \sim 0.5$ in the [110] direction for the fastest electrons of the limiting point. In the [001] direction, the fastest are also the electrons of the limiting point with u/u_0 0.3. The electrons of the orbits passing through the closed ring of four tubes have in all probability no appreciable value of u/u_0, since these orbits are close to the central section, owing to the narrowness of the necks between the tubes.

At the same time, a relatively small contribution of the electrons of the third band to the helicon damping

can be noticed as a result of the quantization of the orbits. In strong fields, quantum oscillations of the impedance were observed, with an amplitude that increased strongly when a standing wave was excited in the metal. Judging from the magnitude of the period $\Delta(1/H)$, these oscillations correspond to the sections of the tubes located in the plane (001) in the third energy band (see[18]), and are not observed when H ‖ [001]. It is interesting that the amplitude of the quantum oscillations of sample 3_1 is very small if H ‖ [110], when the corresponding section of the tube is located parallel to the surface of the sample, and is large if the angle between H and [110] is $\gtrsim 30°$, when the oscillations are determined by the sections of the tubes directed along [110]. Thus, in accordance with the theory of Miller and Kwok[19], the quantum oscillations of the helicon damping are due to electrons whose trajectories do not lie in a plane perpendicular to k. Quantum oscillations were observed earlier in investigations of helicons[20].

SIZE EFFECTS IN A NORMAL FIELD

1. In fields $H < H_e$, sinusoidal oscillations were observed, periodic in the straight field, with a period ΔH that did not depend on the frequency of the external electromagnetic field and was inversely proportional to the thickness of the sample. Apparently this oscillatory size effect is connected with motion of a certain group of electrons along a helix to the interior of the metal. A typical plot of the oscillations in the case of H ‖ [001] is shown in Fig. 13. With increasing frequency, the phase of the α-oscillations changes. When the frequency changes from 1 to 3 MHz, the phase shift is $\approx \pi$. In addition, the magnitude of the magnetic field at which the α-oscillations of maximum amplitude are observed turns out to be approximately proportional to $\omega^{1/3}$. This frequency dependence and numerical estimates show that the condition for the observation of the maximum of the amplitude of the long-period α-oscillations is $u \sim \delta$. Here $u = u(H)$ is the displacement for the given group of electrons and δ is the depth of the skin layer, the magnitude of which can be estimated from the width of the lines of the size effect on the effective electrons[11]. We note that δ is larger by 10−15 times than the analogous parameter that serves as the depth of the skin layer in[7]. At 1.5 MHz, the relative line width $\sim \delta/d$ amounts to [1]) $\approx 7\%$, and the condition $u \sim \delta$ is satisfied at H = 13 kOe. The relation $u \sim \delta$ is apparently equivalent to the condition of resonant interaction of the given group of electrons with that harmonic of the alternating field, which has the maximum amplitude.

The magnitude of the observed period ΔH_α makes it possible to assume that the α-oscillations are due to sections of the hole surface. However, whereas for helicons the threshold of the absorption is actually determined by the electrons with extremal value $u = u_{max}$, for the oscillations, as is clear from a comparison of the experimental values of u/u_0 listed in the table and from the plots of Fig. 7, this is not the case. The dis-

FIG. 13. Oscillations of the size effect at H ‖ [001]; sample 1', T = 3.25°K.

crepancy is particularly large for the orientation H ‖ [001]. Apparently, a role is played here by the relative number of electrons having a specified displacement u. In the approximation of almost free electrons, this quantity is proportional to $(\partial u/\partial p_H)^{-1}(T/T_0)$, and in accordance with Fig. 7, the number of electrons causing the α-oscillations at H ‖ [001] is approximately three times larger than that of the electrons with $u = u_{max}$. With the aid of analogous considerations we can explain the selection of orbits causing the oscillations also for the orientation H ‖ [110] or H ‖ [011].

In weak fields at H ‖ [001], narrow peaks (β) have been observed (see Fig. 13), which go over into harmonic β-oscillations in a certain range of fields, shifting in proportion to $\omega^{1/3}$ with increasing frequency. A similar picture was observed in the case of the size effect on the electrons of the limiting point in an inclined field[6]. With increasing magnetic field, the narrow periodic peaks broadened, and went over into sinusoidal oscillations, when the characteristic dimension of the trajectory of the electrons becomes comparable with the depth of the skin layer (see Fig. 11 in[6]). However, for β-oscillations the period ΔH_β turns out to be one-third the β-peak period coinciding with ΔH_α. The ratio $\Delta H_\alpha/\Delta H_\beta = 3$ is satisfied, within the limits of experimental error, for two samples 1' and 1" of different thickness (all the values are listed in the table). On going over to the thicker sample 1, the condition $\Delta H_\beta \sim 1/d$ is violated. The causes of this phenomenon are not clear to us. It is possible that the transition of the β peaks into oscillations with one period or another depends on the ratio δ/d.

The α and β oscillations with a period ratio $\Delta H_\alpha/\Delta H_\beta \approx 3$ were observed also when H ‖ n ‖ [011]. At the same time, at the orientation H ‖ [110] the ratio is different. It should be noted that the accuracy with which ΔH is determined is low, since we were able to observe relatively few numbers. In addition, the study of the α- and β-oscillations is made difficult by the fact that the oscillations that were distinctly sinusoidal in shape were

---

[1]) In [11], δ was estimated to be half as large. This is apparently not justified, since only the emergence of the peak of the alternating field to the opposite surface of the plate is important in the first approximation.
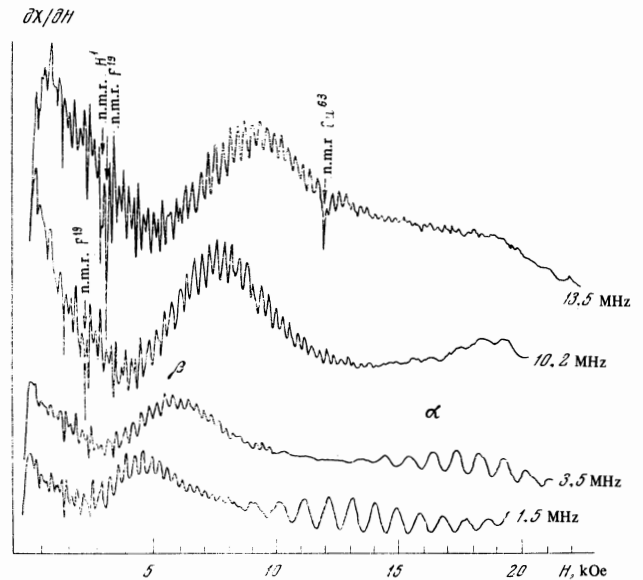
observed in a narrow angular interval near the rational crystallographic directions. Thus, in samples 1' or 1", with H inclined several degrees to [001] the period of the α- and β-oscillations remains unchanged, but the amplitude decreases rapidly (the existence interval is $\pm 4°$). The amplitudes of the oscillations and of the helicons are maximal at the same field direction. For samples of other orientations, the direction of H along the crystallographic axis was also determined from the maximum of the helicon amplitude. When H deviated from the [110] axis in the case of samples 3, or from the [011] axis in the case of sample 4, we observed a complicated interference picture instead of sinusoidal oscillations. It was impossible to determine the laws governing the variation of the periods. It could only be noted that when H was rotated by $\approx 5°$ relative to [110] in the $(1\bar{1}0)$ plane the main period ΔH_α apparently increased by 15–20%, and remained unchanged with further increase of the angle. The same holds for sample 4 when H is rotated in the $(01\bar{1})$ plane.

We can propose two different explanations of the β-oscillations. First, they may be due to certain small groups of electrons, for example the sections of the tubes in the third bands. When H ‖ [001] or H ‖ [110], the orbits of the electrons of the third band, for which u/u_0 corresponds in accordance with the estimates to the experimentally observed period ΔH_β, are strongly elongated along the tube axis. Therefore the indicated assumption is favored by the fact that when H ‖ n ‖ [110] the harmonic β-oscillations could be observed with certainty only at E ‖ [001] (if E ‖ [$\bar{1}$10], then a complicated interference pattern is observed, in which it is impossible to separate oscillations of any definite period). At the same time, there are many circumstances which cast doubts on the hypothesis advanced above. The extremum of u/u_0 for orbits on tubes is apparently reached only at the limiting points. At the same time, the electrons of the limiting points do not lead to noticeable oscillations in the case of the hole surface. Further, when H ‖ [011], the extremum of u/u_0 is reached on a certain intermediate section of the tube, but show that the value $u/u_0 \approx 0.05$ for this section is too small. Finally, when H ‖ [001], the β-oscillations go over into individual in weak fields, and the period of the β peaks in samples 1' and 1" coincides with ΔH_α within the limits of experimental error. The latter circumstance justifies another hypothesis, according to which the β-oscillations are due to the same orbits as the α-oscillations.

As indicated by Gantmakher and Kaner[7], the presence of higher harmonics in the Fourier expansion of the transverse components of the electron velocity

$$v_x = \sum_n v_n' \cos n\Omega t, \qquad v_y = \sum_n v_n'' \sin n\Omega t$$

leads to the appearance of higher harmonics with wave numbers $2\pi n/u$ in the distribution of the field penetrating into the metal as a result of motion of this group of electrons. If the section p_H = const has two perpendicular planes of mirror symmetry x = 0 and y = 0 then, in accordance with the general properties of Fourier series, there are no even harmonics in the expansions of v_x and v_y. Thus, one cannot exclude the possibility that oscillations, corresponding to the third harmonic in

the field distribution, which is excited when $u/3 \sim \delta$, were observed at H ‖ [001] and H ‖ [011]. This scheme does not account for the β-oscillations at H ‖ [110], which correspond more readily to the fifth harmonic.

The question of the nature of the short-period oscillations calls for further study. It would be interesting in this connection to observe oscillations of the size effect in In with the aid of a procedure in which there is no skin layer, for example by measuring the static conductivity[21] or with the aid of point contacts[22]. It is also desirable to perform measurements on other metals with a known Fermi surface.

We were unable to observe oscillations in samples for which H ‖ n ‖ [100]. As to the orientation H ‖ [111], in sample 5 we observed frequency-independent very weak oscillations with amplitudes on the order of the noise level. Judging from the value of the period given in the table, they are due to limiting-point electrons on the large spherical part of the Fermi surface in the [111] direction. However, these oscillations were not seen observed in the thinner sample 5'. We observed instead oscillations of much smaller period, corresponding to mixing of another group of electrons. Thus, just as in the case of Sn, we were unable to observe reliably oscillations from the limiting-point electrons. This result is quite natural, if account is taken of the fact that the electrons of the vicinity of the limiting point travel almost perpendicularly to the high frequency field and acquire a small velocity increment.

2. In samples 1' and 1", we observed besides the β peaks, in weak fields and at low temperatures, an additional series of size-effect lines, which we denoted by the letter γ. The γ-lines differ from the α- and β-lines primarily in their temperature dependence. When the temperature of sample 1' is decreased from 3.5 to 1.4°K, the amplitude of the α- and β-oscillations increased by approximately six times, whereas that of the γ-line increased by 30 times. At low temperature, as a result of interference of two groups of lines, the picture of the size effect in the normal field becomes much more complicated. In the remaining samples, the γ-lines were observed only when H ‖ [100]. There were no oscillations for this field orientation, and the study of the γ-lines was simplified. All the experimental facts give grounds for assuming that the γ-lines are due to effective electrons having a large displacement along the field within the cyclotron period. For the H ‖ [001] or H ‖ [100] orientation, such properties are possessed by orbits passing through the rectangular "cups" of the Fermi surface of the second band. For example, the electrons of cross section a (Fig. 6) move in segment 1 almost parallel to the surface of the sample with n ‖ [001], while in segment 2 they have $v_H \sim v_f$. The trajectory of this group of electrons in real space is a "staircase" in which the horizontal "platforms" follow every quarter of complete revolution. At E ‖ [110], the size-effect lines enable us to register the fact that an integer number of spans of the "staircase" fit in the sample. If E ‖ [100], then only lines corresponding to the path between two parallels "platforms" should remain.

The experimental curves shown in Fig. 14 confirm these considerations. On curve 1, the peaks γ_1 and $\gamma_{1/2}$ are much larger than the peaks $\gamma_{3/4}$ and $\gamma_{1/4}$, and at
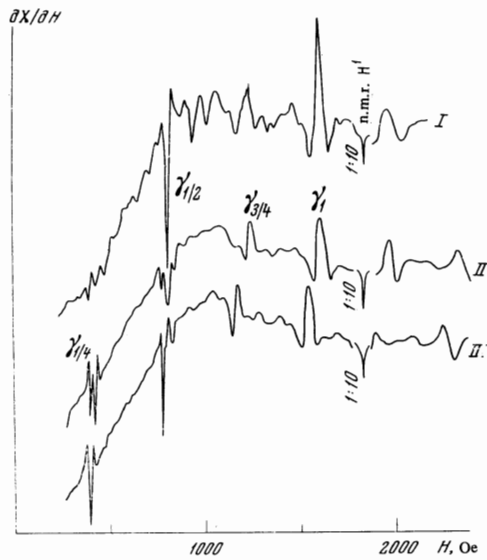
FIG. 14. Effective-electron size-effect lines: $T = 1.6°K$, $\omega/2\pi = 7.8$ MHz. Curve I—sample $2'_2$, $E \parallel [010]$, $H \parallel [100]$; curve II—sample $2'_1$, $E \parallel [011]$, $H \parallel [100]$; curve III—sample $2'_1$, $1.5°$ angle between H and $[100]$. The sensitivity was decreased by 10 times in the plots of the nuclear resonance.

$E \parallel [011]$ the amplitude of all the lines is approximately the same. The table lists the value of the field H_γ corresponding to the start of the line γ_1.

The γ-lines are very sensitive to the change of the angle between the magnetic field and the crystallographic directions. The line γ_1 shifts with increasing φ to weaker fields, and the relative change of the field H_γ is of the order of 10% at $\varphi \approx 10°$. The value $\varphi = 0$ corresponds to the maximum amplitude of the helicons. The γ_1 line shape does not change in the interval $\pm 15°$. At larger inclinations, additional peaks appear, and the picture becomes much more complicated.

Other γ-lines react to small changes of φ in a more complicated manner. For example, in sample $1'$ at $E \parallel [010]$ the line $\gamma_{1/2}$ shifts if H is rotated in the (100) plane, and splits if H is inclined relative to the [001] axis in the (010) plane. This can be readily explained by means of the geometry of the Fermi surface. In both cases, an important role is played by the displacement of the electron along the field during the transit time between two parallel "platforms," where the electron shifts along E. If H deviates from the axis in a plane perpendicular E, then the values of the displacement will be different for the two halves of the total orbit shown dashed in Fig. 6, since v_H is smaller in Section 2 than in Section $2'$.

In samples $1''$ and $2'$, split lines were observed even in a field parallel to the crystallographic axis (see Fig. 14, curve II). This circumstance is apparently due to the rather large asymmetry of the orientations of these samples. However, it was possible to observe unsplit lines at a definite rotation angle of the field relative to the crystal axis (curve III, Fig. 14).

We make one remark concerning the influence of electron scattering on the oscillation amplitude. The length of the trajectory at a fixed value of the displacement along the field is determined by the ratio of p/T_0 to u/u_0. For $H \parallel [001]$, according to the diagrams of

Fig. 7, the length of the trajectory is minimal when $p_H = 0$ and increases with increasing p_H. From H_γ we can determine the corresponding value of $p_H = 0.15$ by using the plot of u/u_0. Thus, the length of the trajectory of the electrons causing the α-oscillations turns out to be larger by 1.2 times than the length of the trajectories for the γ-lines. At the same time, in the investigated temperature range $1.4-4°K$, the amplitude of the oscillations depends on the temperature less than the amplitude of the γ-lines. In addition, the γ-lines were not observed in the thick sample 1. This means that the mean free path of the electrons turns out to be smaller for the γ-lines than for the oscillations. Obviously, for the effective electrons a small-angle deflection following scattering by the phonons is more significant than for the ineffective electrons.

CONCLUSION

Greatest interest, from our point of view, attaches to the following results of our investigation.

1. Weakly-damped helical waves are observed in In when $ku_0 = 2\pi$, i.e., when the condition of the Doppler-shifted cyclotron resonance is satisfied for the electrons of the limiting points, the presence of which follows from other experimental data. On the other hand, in alkali metals the threshold of helicon absorption is determined precisely by the electrons of the limiting point. This contradiction can be qualitatively explained as follows. If $H > H_e$, then the damping of the helicons is small and the wave is characterized by a definite value of k. When the condition $ku_0 = 2\pi$ is satisfied, the damping increases as a result of the resonant interaction of the wave with the limiting-point electrons, and the spectrum of the wave vectors of the helicons becomes smeared out. This in turn makes it possible for the electrons of the near-lying sections with $u < u_0$ to come into play, so that as a net result all the electrons interact with the electromagnetic field, which is described by an infinite set of wave vectors and attenuates rapidly within the metal (skin effect). In indium, the electrons of the limiting points are isolated, so that they increase the helicon damping only slightly, and the absorption threshold in the field H_e is determined by other extremal sections.

2. For the orientation $H \parallel [100]$, besides ordinary helicons, we observed a wave propagating in a metal when $H < H_e$. We were unable to explain it with the aid of the presently known considerations.

3. A qualitative explanation was presented for the observed dependences of the amplitude of the helicons in indium on the direction of magnetic field by taking into account the Landau damping. Under the conditions of our experiments, this damping mechanism comes into play if there exist central-section electrons whose trajectories do not lie in a constant-phase plane of the wave, regardless of the mutual orientation of H and k.

4. On the basis of the result of an investigation of the size-effect oscillations due to the ineffective electrons, it is concluded that the oscillations of largest magnitude are observed under conditions of resonant interaction between electrons and that harmonic of the alternating field in the skin layer, which has the maximum amplitude. Short-period oscillations were observed which

were apparently connected with the anomalous penetration of higher harmonics of the field distribution within the metal.

5. In relatively weak fields we observed, besides the oscillations, also narrow size-effect lines in the normal field, due to the effective electrons.

The author is grateful to P. L. Kapitza for the opportunity of performing the work at the Institute of Physics Problems, and to V. F. Gantmakher and Yu. V. Sharvin for a detailed discussion of the results and valuable advice.

[1] É. A. Kaner and V. G. Skobov, Usp. Fiz. Nauk 89, 367 (1966) [Sov. Phys.-Usp. 9, 480 (1967)].

[2] Plasma Effects in Solids, Dunod, Paris, (1965), pp. 3—35.

[3] M. T. Taylor, Phys. Rev. 137, A1145 (1965).

[4] J. L. Stanford and E. A. Stern, Phys. Rev. 144, 534 (1966).

[5] G. Weisbuch and A. Libchaber, Phys. Rev. Lett. 19, 498 (1967).

[6] V. F. Gantmakher, Progr. in Low Temperature Phys. 5, 181 (1967).

[7] V. F. Gantmakher and É. A. Kaner, Zh. Eksp. Teor. Fiz. 48, 1572 (1965) [Sov. Phys.-JETP 21, 1053 (1965)].

[8] V. F. Gantmakher and I. P. Krylov, ibid. 49, 1054 (1965) [22, 734 (1966)].

[9] R. T. Mina and M. S. Khaĭkin, ibid. 51, 62 (1966) [24, 42 (1967)].

[10] V. F. Gantmakher, ibid. 44, 811 (1963) [17, 549 (1963)].

[11] I. P. Krylov and V. F. Gantmakher, ibid. 51, 740 (1966) [24, 492 (1967)].

[12] C. R. Legendy, Phys. Rev. 135, A1713 (1964).

[13] R. G. Chambers and B. Jones, Proc. Roy. Soc. A270, 417 (1962).

[14] G. N. Harding and P. C. Thonemann, Proc. Phys. Soc. 85, 317 (1965).

[15] J. J. Quinn and S. Rodriquez, Phys. Rev. 133, A1589 (1964).

[16] J. C. McGroddy, J. R. Stanford, and E. A. Stern, Phys. Rev. 141, 437 (1966).

[17] P. Antoniewicz, Phys. Lett. 24A, 83 (1967).

[18] G. B. Brandt and J. A. Rayne, Phys. Rev. 132, 1512 (1963).

[19] P. B. Miller and P. C. Kwok, Phys. Rev. 161, 629 (1967).

[20] C. C. Grimes, Plasma Effects in Solids, Dunod, Paris, (1965), p. 87.

[21] P. D. Hamburger, J. A. Marcus, and J. A. Munarin, Phys. Lett. 25, 461 (1967).

[22] Yu. V. Sharvin and L. M. Fisher, ZhETF Pis. Red. 1, No. 5, 54 (1965) [JETP Lett. 1, 152 (1965)].

Translated by J. G. Adashko
202